Molecular Pharmacology Fast Forward. Published on September 1, 2016 as DOI: 10.1124/mol.116.105437
This article has not been copyedited and formatted. The final version may differ from this version.

TITLE PAGE

The selective $Na_v1.7$ inhibitor, PF-05089771, interacts equivalently with fast and slow inactivated $Na_v1.7$ channels

Jonathan W. Theile, Matthew D. Fuller and Mark L. Chapman

Pfizer Neusentis US, Pfizer Global Research Unit of Pfizer Ltd (Currently, Icagen, Inc.)

Icagen, Inc. (JWT, MDF, MLC)

Molecular Pharmacology Fast Forward. Published on September 1, 2016 as DOI: 10.1124/mol.116.105437
This article has not been copyedited and formatted. The final version may differ from this version.

RUNNING TITLE PAGE

a) Running title: Biophysical profiling of $Na_v1.7$ inhibitor, PF-05089771

b) Correspondence:

Jonathan Theile

Icagen, Inc.

4222 Emperor Boulevard, Suite 350

Durham, North Carolina 27703

United States

Tel: (919) 941-5206

FAX: (919) 941-0813

jtheile@icagen.com

c) Manuscript counts:

Text pages: 32

Figures: 5

Tables: 1

References: 32

Abstract: 243

Introduction: 664

Discussion: 1094

d) Abbreviations: DI-DIV, domains I-IV; DMSO, dimethyl sulfoxide; HEK293, human embryonic kidney 293; Na_v, voltage-gated sodium channels; PM, pore module; S1-S6, transmembrane segments 1-6; VSD, voltage-sensing domain

Molecular Pharmacology Fast Forward. Published on September 1, 2016 as DOI: 10.1124/mol.116.105437
This article has not been copyedited and formatted. The final version may differ from this version.

Abstract

Voltage-gated sodium (Na_v) channel inhibitors are used clinically as analgesics and local anesthetics. However, the absence of Na_v channel isoform selectivity of current treatment options can result in adverse cardiac and central nervous system side effects, limiting their therapeutic utility. Human hereditary gain- or loss-of-pain disorders have demonstrated an essential role of $Na_v1.7$ sodium channels in the sensation of pain, thus making this channel an attractive target for new pain therapies. We have previously identified a novel, state-dependent human $Na_v1.7$ selective inhibitor (PF-05089771, IC_{50} = 11 nM) that interacts with the voltage-sensor domain (VSD) of Domain IV. We have further characterized the state-dependent interaction of PF-05089771 by systematically varying the voltage, frequency and duration of conditioning prepulses to provide access to closed, open and fast- or slow-inactivated states. The current study demonstrates that PF-05089771 exhibits a slow onset of block that is depolarization- and concentration-dependent, with a similarly slow recovery from block. Furthermore, the onset of block by PF-05089771 develops with similar rates using protocols that bias channels into predominantly fast- or slow-inactivated states, suggesting that channel inhibition is less dependent on the availability of a particular inactivated state than the relative time that the channel is depolarized. Taken together, the inhibitory profile of PF-05089771 suggests that a conformational change in the Domain IV-VSD following depolarization is necessary and sufficient to reveal a high affinity binding site with which PF-05089771 interacts, stabilizing the channel in a non-conducting conformation from which recovery is slow.

Molecular Pharmacology Fast Forward. Published on September 1, 2016 as DOI: 10.1124/mol.116.105437
This article has not been copyedited and formatted. The final version may differ from this version.

Introduction

Voltage-gated sodium (Na_v) channels play a key role in regulating action-potential generation and propagation in excitable cells (Hodgkin and Huxley, 1952). The Na_v channel is a heteromeric protein complex consisting of a pore-forming α-subunit and auxiliary β-subunits (Catterall, 2000). The α-subunit consists of four homologous domains (DI-DIV), each containing six membrane spanning segments (S1-S6). The S1-S4 segments together comprise the voltage-sensing domain (VSD), in which translocation of the positively charged S4 segment following depolarization plays a critical role in the initiation of voltage-dependent gating (Catterall, 2010; Noda et al., 1984; Stuhmer et al., 1989). The S5-S6 segments of each domain converge to form the ion conducting pore module (PM), with the residues along the S6 segment constituting the inner pore (Ragsdale et al., 1994).

Inhibitors selective for peripherally expressed $Na_v1.7$, $Na_v1.8$ and $Na_v1.9$ isoforms have been identified as potential analgesics for the treatment of pain (Dib-Hajj et al., 2009; Payne et al., 2015; Theile and Cummins, 2011), particularly $Na_v1.7$ (Alexandrou et al., 2016; Cox et al., 2006; Dib-Hajj et al., 2008). Current pharmacological treatments for pain which demonstrate activity against Na_v channels include local anesthetics, tricyclic antidepressants, and anticonvulsants, however many of these treatment options do not provide adequate pain relief and exhibit adverse central nervous system and cardiac toxicities, presumably due to a lack of pharmacological selectivity across the Na_v family (Cummins and Rush, 2007). These classical Na_v channel blockers bind to conserved residues along the pore-forming S6 segment of the Na_v channel resulting in little to no selectivity amongst Na_v channel subtypes (Ragsdale et al., 1994, 1996; Yarov-Yarovoy et al., 2001, 2002). The typically narrow therapeutic index of classical Na_v blockers is attributable to a degree of functional selectivity achieved through state- and/or

Molecular Pharmacology Fast Forward. Published on September 1, 2016 as DOI: 10.1124/mol.116.105437
This article has not been copyedited and formatted. The final version may differ from this version.

frequency-dependent inhibition (Fozzard et al, 2005). Thus, there exists a need for the development of small molecule inhibitors with novel binding properties and Na_v channel subtype selectivity in order to enhance clinical utility while minimizing undesired side effects. As gating modifier toxins have been shown to affect normal voltage-dependent gating of Na_v channels through an interaction with less conserved extracellular residues of the VSD and the nearby PM (Catterall et al., 2007; Wang et al., 2011; Xiao et al., 2014), the development of small molecules which alter VSD function may display improved specificity and isoform selectivity over current treatment options.

We recently reported a class of low nanomolar-potency, state-dependent Na_v inhibitors which bind to a novel site on the VSD of DIV, conferring a high degree of selectivity amongst Na_v isoforms (McCormack et al., 2013). Within this class of aryl sulfonamide small molecules, PF-05089771 is a novel, selective and potent human $Na_v1.7$ inhibitor, exhibiting an IC_{50} of ~11 nM for inactivated channels (Alexandrou et al., 2016). In addition to the potency and selectivity, PF-05089771 was reported to be distinguished by its strong preference for inactivated channels and the slow rate at which inhibition develops. In that initial report by Alexandrou and colleagues, it was observed that long applications of compound were required to achieve steady-state inhibition of $Na_v1.7$ channels at concentrations near the IC-50. One possible interpretation of this observation is that PF-05089771 exhibits a preference for a slow-inactivated state of the channel that accumulates with repeated activation. However the previous series of experiments did not directly address the possibility of slow association with multiple inactivated conformations. In this report, we sought to differentiate between these possibilities by altering the relative availability of the various kinetic states of the channel. We investigated this question using voltage-clamp protocols which biased channels into predominantly fast- or slow-

Molecular Pharmacology Fast Forward. Published on September 1, 2016 as DOI: 10.1124/mol.116.105437
This article has not been copyedited and formatted. The final version may differ from this version.

inactivated state populations. We observed that inhibition occurs following depolarization of the channel, with the time course for inhibition largely unaffected by the relative availability of either open or kinetically distinct inactivated states. These results indicate that depolarization of the channel into a non-resting conformation is the primary determinant for PF-05089771-mediated inhibition, and any subsequent conformational changes associated with the progressive development of inactivation did not substantially alter the interaction of PF-05089771 with the channel.

Molecular Pharmacology Fast Forward. Published on September 1, 2016 as DOI: 10.1124/mol.116.105437
This article has not been copyedited and formatted. The final version may differ from this version.

Materials and Methods

Reagents

PF-05089771 [2,2-diphenyl-N-(4-(N-thiazol-2-ylsulfamoyl)phenyl)acetamide] was synthesized by the medicinal chemistry group at Neusentis, Durham, NC (Alexandrou et al., 2016).

Cell culture

Human $Na_v1.7$ was stably expressed in human embryonic kidney 293 cells (HEK293) cells. Methods of stable cell line generation were as described in McCormack et al., 2013.

Electrophysiology

Cover slips with HEK293 cells expressing human $Na_v1.7$ were placed in a recording chamber on the stage of an inverted microscope and perfused with an extracellular solution containing (in mM), 132 NaCl, 1.8 $CaCl_2$, 5.4 KCI, 0.8 $MgCl_2$, 5 glucose, and 10 HEPES, pH 7.4, with NaOH. Recording patch pipettes were filled with an intracellular solution containing (in mM), 110 CsF, 35 CsCl, 5 NaCl, 10 EGTA, 10 HEPES, pH 7.3 with CsOH, and had a resistance of 1 to 3 MΩ. All reagents used for buffers were purchased from Sigma-Aldrich (St. Louis, MO). All recordings were made at room temperature (22-24°C) using Axopatch 200B or Multiclamp 700B amplifiers and PCLAMP software (Molecular Devices, Sunnyvale, CA). Sodium currents were measured using the whole-cell configuration of the patch-clamp technique. All compounds were dissolved in dimethyl sulfoxide (DMSO) to make 10 mM stock solutions, which were then diluted into extracellular solution to attain the final concentrations desired. The final concentration of DMSO (<0.1%) was found to have no significant effect on sodium currents. Assessment of recovery from inactivation and development of inhibition in the presence of PF-05089771 are described in the text and figure legends.

Molecular Pharmacology Fast Forward. Published on September 1, 2016 as DOI: 10.1124/mol.116.105437
This article has not been copyedited and formatted. The final version may differ from this version.

Data analysis

Data were analyzed using the software programs of Clampfit 10.3 (Molecular devices) and GraphPad Prism 6.0 (GraphPad Software, Inc., San Diego, CA). Statistical analysis was calculated by Student's *t* test or ANOVA where mentioned, and $P < 0.05$ indicates a significant difference. All data are presented as mean ± SEM, and error bars in figures represent SEM.

Peak inward currents obtained from activation protocols were converted to conductance values using the equation, $G=I/(V_m - E_{Na})$, for which G is the conductance, I is the peak inward current, V_m is the membrane potential step used to elicit the response, and E_{Na} is the reversal potential for sodium (determined for each cell using the x-axis intercept of a linear fit of the peak inward current responses). Conductance data were normalized by the maximum conductance value and fit with a Boltzmann equation of the form $G = G_{min} +(G_{max} - G_{min})/(1 + \exp[(V_{1/2} - V_m)/k)]$, where $V_{1/2}$ is the midpoint of activation, and k is a slope factor. Peak inward currents obtained from steady-state inactivation protocol were normalized by the maximum current amplitude and fit with a Boltzmann equation of the form $I = I_{min} + (I_{max}- I_{min})/(1+\exp[(V_m - V_{1/2})/k)]$, where V_m represents the inactivating prepulse membrane potential, and $V_{1/2}$ represents the midpoint of inactivation.

Recovery from inactivation was well described by a sum of two exponential components, and the development of inhibition in the presence of PF-05089971 was well described using a one phase decay. A 'plateau followed by a one phase decay' was employed for datasets where there was a steady-state baseline region prior to application of the compound. For experiments measuring the recovery from inactivation in the absence of PF-05089771, averaged data for each group was fit. For experiments measuring the development of inhibition in the presence of PF-

Molecular Pharmacology Fast Forward. Published on September 1, 2016 as DOI: 10.1124/mol.116.105437
This article has not been copyedited and formatted. The final version may differ from this version.

05089771 and recovery from inhibition during washout of PF-05089771, individual cells were fit to provide the time constants, which were averaged and shown as mean ± SEM.

Molecular Pharmacology Fast Forward. Published on September 1, 2016 as DOI: 10.1124/mol.116.105437
This article has not been copyedited and formatted. The final version may differ from this version.

Results

PF-05089771 displays state-dependent inhibition of hNa$_v$1.7 currents. PF-05089771 has previously been shown to produce potent and selective inhibition of human Na$_v$1.7 (IC_{50} 11 nM) using a voltage protocol with a conditioning prepulse that evenly distributes the channel population across resting closed and inactivated states (Alexandrou et al., 2016). In the current study we examined in more detail the kinetics and state dependence of this interaction using the same protocol, which consists of an 8 s conditioning voltage step to an empirically determined membrane potential that results in 50% inactivation for each cell followed by 2 ms hyperpolarizing pulse to -120 mV to partially relieve inactivation and then a 20 ms test pulse to 0 mV (Figure 1A, *right inset*). This voltage protocol results in channels in both the fast and slow inactivated states which reach equilibrium during the progression of the pulse train (sweep interval of 15 s). At 100 nM PF-05089771, a concentration ~9-fold higher than the previously reported IC_{50}, hNa$_v$1.7 currents are fully inhibited with a time constant of 212 ± 17 s (n=3, Figures 1A-B). The rate of inhibition at 1 μM, develops more rapidly, with a time constant of 33 ± 1 s (n=9). Figures 1A-B also show that in the absence of an 8 s conditioning voltage step to promote inactivation, little or no inhibition during a 17 minute exposure to 100 nM PF-05089771 was observed, which is consistent with previously reported a lack of interaction with resting closed channels (Alexandrou et al., 2016).

To investigate the time course of PF-05089771 unblock that occurs when channels are returned to the resting closed state (i.e. at -120 mV), we applied the half-inactivation protocol described above until maximal inhibition was established and then switched to a holding potential of -120 mV, applying a 20 ms test pulse every 10 s to assess magnitude of current recovery during washout of the compound. Recovery of current was slow (τ = 526 ± 36 s, n=5)

Molecular Pharmacology Fast Forward. Published on September 1, 2016 as DOI: 10.1124/mol.116.105437
This article has not been copyedited and formatted. The final version may differ from this version.

and incomplete, with current amplitude recovering slightly less than 60% of the pre-drug levels after 15 minutes. (Figure 1C). Failure to recover 100% of the current even after nearly 20 minutes may be partially due to rundown of the current over time.

Using brief depolarizations, PF-05089771 exhibits very slow use-dependent block of $hNa_v1.7$ except at very high concentrations. As the presence or absence of use-dependent block can provide a measure for the relative affinity for the open/fast-inactivated state, we assessed use-dependent inhibition by PF-05089771 using a 10 s high frequency pulse train consisting of 100 steps (20 ms) to 0 mV at a rate of 10 Hz. As seen in Figure 2A, we observed no difference between the DMSO control and 100 nM of PF-05089771, a concentration ~9-fold higher than the published IC_{50} for partially inactivated channels (Alexandrou et al, 2016). Only at 10 µM (~900-fold over IC_{50}) do we observe complete use-dependent block with a single 10 Hz train for 10 s. At concentrations less than 10 µM, in excess of 100 pulses at 10 Hz was needed to achieve steady-state inhibition (data not shown). Following complete block with 10 µM PF-05089771, the currents were then allowed to recover in the absence of compound using the resting channel protocol (Figure 2B). Currents recovered to at a similar rate (633 ± 57 s) but to a greater extent (about 75% of the pre-drug amplitude) within the same time frame as shown in Figure 1C. The greater extent of current recovery may be partially explained by the ~6 minutes shorter overall recording time (block and recovery) used for the experiment in Figure 2, thus minimizing the contribution of current rundown. The requirement of such high concentrations to observe use-dependent block could be attributable to a low affinity of PF-05089771 for the open/fast-inactivated state, and/or the need to overcome the very slow apparent on-rate of the compound. In the following sections, we explored this question by testing the relative affinity

Molecular Pharmacology Fast Forward. Published on September 1, 2016 as DOI: 10.1124/mol.116.105437
This article has not been copyedited and formatted. The final version may differ from this version.

for the fast- versus slow-inactivated states using voltage-clamp protocols that also account for the slow recovery from block of the compound.

Investigating the development of inhibition for fast- and slow-inactivated channels. Thus far the data presented in Figures 1 and 2 show that the kinetics of and recovery from inhibition of $hNa_v1.7$ by PF-05089771 are slow, with brief depolarizations (Fig 2) resulting in no appreciable inhibition, even at a concentration 9-fold higher than the IC_{50} for inactivated channels. However, these observations do not rule out the possibility of slow binding to fast-inactivated channels. In an effort to understand the mechanism of inhibition, we employed several voltage-clamp protocols that biased channels into predominantly fast- or slow-inactivated populations and subsequently measured the onset of inhibition by 100 nM PF-05089771.

We first determined the availability of fast- versus slow-inactivated states in the absence of PF-05089771 using inactivating step depolarizations to 0 mV for durations of 0.1, 1, 4 or 8 s followed by a hyperpolarizing step to -120 mV for increasing durations to assess recovery from inactivation. As seen in Figure 3A, the recovery from inactivation was well described by a sum of two exponential components with the shorter conditioning pulses increasing the relative availability of the fast-inactivated state (see Table 1). Not until the 4 and 8 s depolarizations do we observe a substantial fraction of the channels entering the slowly recovering state.

To assess channel inhibition following either a short (1 s) or long step (8 s) to 0 mV, we used a fixed recovery interval of 1 and 3 s at -120 mV, respectively. These recovery intervals allowed for a similar amount of current to be recovered (~93% available) in the absence of any compound ensuring that the current amplitude remained stable under control conditions for both protocols. Importantly, the 1 and 3 s recovery intervals were still sufficiently brief to not allow any appreciable recovery from PF-05089771 mediated inhibition. The compound was perfused

Molecular Pharmacology Fast Forward. Published on September 1, 2016 as DOI: 10.1124/mol.116.105437
This article has not been copyedited and formatted. The final version may differ from this version.

until inhibition stabilized. As shown in Figure 3C, plotting the fraction of available current over total time (time at 0 mV and -120 mV), the block develops 4.5-fold faster for the 8 s pulse to 0 mV (τ = 65 ± 5 s, n=7), compared to the 1 s pulse to 0 mV (τ = 304 ± 34 s, n=5). If PF-05089771 interacts preferentially with the slow-inactivated state, this result could be explained by the higher fraction of channels in the slow-inactivated state (88%) following the 8 s step to 0 mV compared to the 1 s step (30%). However, this initial assessment does not take into account the fraction of the total time spent at rest when little or no block is expected to occur. Therefore, the data were re-plotted as the fraction of available current as a function of the total time spent at 0 mV (Figure 3E). When reanalyzed in this manner the rate of block between both protocols was found to be indistinguishable (τ = 31 ± 1 s vs 32 ± 4 s for the 8 s and 1 s conditioning steps, respectively; $P > 0.05$ by unpaired t-test). Thus, the apparent slower rate of block seen with the shorter conditioning pulse in Figure 3C can be explained by the briefer availability (1 versus 8 s) of the depolarized state with which PF-05089771 can interact. These results suggest that the relative availability of slow versus fast-inactivated channels has less of an impact on the development of inhibition than the total time spent in the depolarized state.

In the second set of experiments to investigate whether PF-05089771 interacts more favorably with slow- or fast-inactivated channels, we employed two protocols in which the total protocol length and time spent at 0 mV prior to the test pulse are identical, but the fraction of channels populating the slow versus fast-inactivated states are different. This was achieved by applying a single conditioning voltage step to 0 mV for 4 s at a frequency of 0.1 Hz or a conditioning train of ten 400 ms steps to 0 mV at a frequency of 1 Hz. At both 0.1 and 1 Hz stimulation frequencies, the cell is depolarized to 0 mV for a total of 4 s prior to the test pulse (Figure 4A, *right*). As shown in Figure 4A (*left*), the recovery from inactivation was well

Molecular Pharmacology Fast Forward. Published on September 1, 2016 as DOI: 10.1124/mol.116.105437
This article has not been copyedited and formatted. The final version may differ from this version.

described by a sum of two exponential components with the 0.1 Hz prepulse (τ_{fast} = 9 ms, A_{fast} = 28%; τ_{slow} = 340 ms, A_{slow} = 72%) providing greater availability of slow inactivated channels as compared to the 1 Hz prepulse (τ_{fast} = 4 ms, A_{fast} = 79 %; τ_{slow} = 162 ms, A_{slow} = 21%). To assess block of the channel following the 0.1 Hz or 1 Hz pre-pulse trains, a fixed recovery interval of 3 s at -120 mV (Figure 4B, *right*) was used for both conditioning protocols as this interval allowed for more than 90% of the current to be recovered in both protocols under control conditions. Again, due to the very slow rate of recovery from inhibition by PF-05089771, the 3 s recovery step between the conditioning pulse(s) and the test pulse is not sufficiently long to allow appreciable recovery from inhibition. As shown in Figure 4B (*left*), the onset of inhibition is indistinguishable using the 1 Hz or 0.1 Hz prepulse (τ = 141 ± 23 s and 178 ± 16 s, respectively, n=3 each; P > 0.05 by unpaired t-test) despite the >3-fold difference in availability of slow inactivated channels. These results provide additional evidence that the relative availability of particular inactivated state conformations has little to no influence on the development of PF-05089771 mediated inhibition.

In the final experiment to investigate whether PF-05089771 displays a preference for a particular inactivated state we systematically varied the inactivating voltage while fixing the duration of the conditioning prepulse to 8 s. We set the conditioning voltage to potentials in which the channels are fully inactivated (0 mV and -60 mV), or ~50% inactivated (V0.5 of inactivation potential). The V0.5 of inactivation potential was determined empirically for each cell immediately prior to testing by running a steady-state inactivation protocol (Figure 5A*i*). Across all cells tested, the average V0.5 of inactivation was -84 ± 1 mV, with $\geq$ 99% of the current inactivated at -60 mV (n=9, Figure 5A). We first assessed the availability of fast- versus slow-inactivated states in the absence of PF-05089771 using an inactivating step depolarization

Molecular Pharmacology Fast Forward. Published on September 1, 2016 as DOI: 10.1124/mol.116.105437
This article has not been copyedited and formatted. The final version may differ from this version.

to 0 mV, -60 mV or the V0.5 potential for 8 s. As shown in Figure 5B (*left*), the recovery from inactivation was well described by a sum of two exponential components with the 8 s prepulse to 0 mV (from Table 1) providing greater availability of slow inactivated channels as compared to the prepulse to -60 mV (τ_{fast} = 11 ms, A_{fast} = 83%; τ_{slow} = 515 ms, A_{slow} = 17 %) or the V0.5 of inactivation (τ_{fast} = 14 ms, A_{fast} = 89%; τ_{slow} = 308 ms, A_{slow} = 11%). These results demonstrate that substantially less slow-inactivation is generated with the steps to -60 mV or the V0.5 potential consistent with previous observations for $Na_v1.3$ (Jo and Bean, 2011).

To assess the rate of block by PF-05089771, a fixed recovery interval of 3 s at -120 mV followed the conditioning pulse and the total sweep duration (20 s) was equal for all three protocols. As shown in Figure 5C, the time constant for the onset of block is similar between the conditioning pulse to 0 mV (τ = 67 ± 4 s, n=7) and -60 mV (τ = 90 ± 7 s, n=5; $P > 0.05$ by ANOVA and Tukey's multiple comparison test, despite the strikingly different recovery profiles seen in Figure 5B. The rate of block was significantly slower using the conditioning pulse to the V0.5 of inactivation (τ = 331 ± 56 s, n=6) than that at either 0 or -60 mV ($P < 0.01$ by ANOVA and Tukey's multiple comparison test). These results provide further evidence that PF-05089771 interacts rather indiscriminately with fast- or slow-inactivated channels and gives further indication that there is little or no interaction with resting channels. Additionally, inactivation at 0 mV proceeds primarily through the open-state, whereas inactivation at -60 mV proceeds primarily through the closed-state, as demonstrated by a lack of inward current generated with a step depolarization to -60 mV (Figure 5A). Therefore, the results in Figure 5C suggest that the rate and magnitude of inhibition is largely independent of the route of entry into the inactivated state, as well as the kinetically defined inactivated state in which the channel resides. The single

Molecular Pharmacology Fast Forward. Published on September 1, 2016 as DOI: 10.1124/mol.116.105437
This article has not been copyedited and formatted. The final version may differ from this version.

commonality between the various protocols to observe channel inhibition is the requirement for a sufficiently strong depolarization to move the channels out of the resting conformation.

Molecular Pharmacology Fast Forward. Published on September 1, 2016 as DOI: 10.1124/mol.116.105437
This article has not been copyedited and formatted. The final version may differ from this version.

Discussion

We have previously reported two human $Na_v1.7$ selective aryl sulfonamide small molecule inhibitors, PF-04856264 (McCormack et al., 2013) and PF-05089771 (Alexandrou et al., 2016) which exhibit strong state-dependence, preferentially inhibiting inactivated channels with $\geq$ 1000-fold higher IC_{50} compared to resting channels. In addition to the pronounced state-dependence and Na_v selectivity an unexplored attribute of these molecules is the apparent slow association and disassociation with $Na_v1.7$. In the present study, we sought to further investigate whether the pronounced degree of state-dependent inhibition by PF-05089771 could be attributed to a preference for a particular inactivated state of the channel.

Commonly used two-pulse protocols which examine the voltage- or time-dependence of fast- versus slow-inactivation cannot reliably differentiate compounds which bind preferentially to slow-inactivated state(s) versus those which associate slowly to inactivated channels, particularly if a compound is present while the channels transition through multiple inactivated states as during a long depolarizing pulse (Karoly et al., 2010; Lenkey et al., 2006). Typically these protocols measure the steady-state shifts in availability of slow- and fast-inactivated states in the presence of a state-dependent blocker. One prerequisite of such protocols is the need to 'reset' the system prior to each successive change in conditioning pulse voltage or duration to avoid the accumulation of block in successive sweeps. The slow onset of inhibition with PF-05089771 coupled with the slow and incomplete washout makes use of such protocols unfeasible. We therefore modified the voltage protocols to take advantage of the unique properties of PF-05089771 and allow more quantitative characterization of PF-05089771 mediated inhibition. Utilizing these protocols it was possible to increase availability of the fast-inactivated state without generating appreciable slow-inactivation. The slow time course of

Molecular Pharmacology Fast Forward. Published on September 1, 2016 as DOI: 10.1124/mol.116.105437
This article has not been copyedited and formatted. The final version may differ from this version.

unblock of PF-05089771 minimized recovery from inhibition between successive sweeps and provided long temporal access (within each sweep) to primarily fast-inactivated channels, thereby allowing us to discern slow binding to a population of channels that are predominantly fast-inactivated.

The results presented here suggest that for the development of PF-05089771-mediated inhibition, the preference for a particular inactivated state (fast and/or slow) appears less critical than the relative time that the channel is depolarized. When accounting for the time that the channel is depolarized, the rate of inhibition by PF-05089771 occurs with a similar time course for channels that reside in either predominantly fast- or slow-inactivated states. Thus, the presentation of a particular inactivated state does not appear to be a prerequisite for association of PF-05089771 with the channel. Likewise, these observations do not posit that PF-05089771 interacts with only fast-inactivated channels, as gating changes that occur with long depolarizations or at more depolarized potentials (both of which are associated with the development of slow-inactivation) do not impede inhibition. As such, we propose that the only requirement for PF-05089771-mediated inhibition is a sufficiently strong depolarization to move the channel out of the resting/closed configuration (for which there is very low affinity). Any subsequent conformational changes associated with fast- or slow-inactivation appear to have little observable effect on the interaction of PF-05089771 with the channel. A caveat to this interpretation is that we are unable to employ a protocol which allows a particular inactivated state to be assessed in isolation, since the assumption that channels populate a single fast- or single slow-inactivated state is an over-simplification and it is likely that the channel moves through a series of intermediate conformational changes during the gating process. Furthermore, it has been proposed that that fast- and slow-inactivation are not mutually exclusive, representing

Molecular Pharmacology Fast Forward. Published on September 1, 2016 as DOI: 10.1124/mol.116.105437
This article has not been copyedited and formatted. The final version may differ from this version.

structurally independent, non-sequential processes with both states potentially existing in the same channel simultaneously (Bezanilla et al., 1982; Vedantham and Cannon, 1998).

Utilizing mutagenesis studies, we previously demonstrated that $Na_v1.7$-selective aryl sulfonamide inhibitors interact with the extracellular surface of the VSD region of DIV (Alexandrou et al., 2016; McCormack et al., 2013), although the precise mechanism for inhibition was not fully understood. Over the years, the use of polypeptide toxins has increased our understanding of the functional significance of the VSD of DIV in channel fast-inactivation (Catterall et al., 2007; Groome, 2014; Hanck and Sheets, 2007). Site-3 toxins, which include α-scorpion toxins and sea anemone toxins, bind to overlapping extracellular residues on the DIV S3-S4 loop, binding with highest affinity at negative membrane potentials where the channel is closed (Catterall et al., 2007). These site-3 toxins impede fast-inactivation by trapping the DIV S4 segment and preventing outward translocation upon depolarization (Rogers et al., 1996; Xiao et al., 2014). At least one of the residues (D1586) of the proposed PF-05089771 binding site, located near the extracellular end of the S3 segment, overlaps with the binding site for site-3 toxins. Thus, it remains a possibility that PF-05089771 employs a similar voltage-sensor trapping mechanism to stabilize a non-conducting conformation of the channel. As it has been suggested that movement of the DIV voltage-sensor following depolarization is necessary and sufficient for inactivation via the open (i.e., strong depolarization to 0 mV) or closed states (i.e., mild depolarization to -60 mV) (Capes et al., 2013), we hypothesize that translocation of the DIV voltage-sensor upon depolarization exposes the high-affinity small molecule binding site and binding of PF-05089771 stabilizes the channel into a non-conducting conformation from which recovery to a resting conformation is slow. A recent study by Ahuja and colleagues provides strong support for this hypothesis. Using a chimeric construct of human $Na_v1.7$ DIV VSD and

Molecular Pharmacology Fast Forward. Published on September 1, 2016 as DOI: 10.1124/mol.116.105437
This article has not been copyedited and formatted. The final version may differ from this version.

the bacterial Na_vAb, they were able to demonstrate through both electrophysiological and crystallographic methods that $Na_v1.7$ aryl sulfonamide inhibitors employ a voltage-sensor trapping mechanism to lock the activated DIV voltage-sensor into the activated conformation and thereby stabilizing a nonconductive conformation of the channel (Ahuja et al, 2015).

Antiepileptics and anticonvulsants provide therapeutic utility via use-dependent inhibition of fast firing neurons typically associated with epileptic seizures and pain (Cummins and Rush, 2007). Alternatively, as sodium channels undergo slow inactivation following sustained depolarizations, neurons which are abnormally depolarized for long periods of time (following injury or insult) may be susceptible to enhanced block via slow-inactivation preferring drugs (Errington et al., 2008; Hildebrand et al., 2011; Jo and Bean, 2011). As PF-05089771 and its congeners interact with the VSD to inhibit depolarized human $Na_v1.7$ channels, irrespective of the channel state, this mechanism of action may provide a therapeutic benefit across multiple types of pain modalities characterized by any type of $Na_v1.7$ channel activity. We believe that the development of small molecules that act as Na_v channel gating modifiers via an interaction with the VSD, as opposed to more classical non-selective inhibitors which bind inside the channel pore, represents an avenue worthy of further exploration in an effort to obtain improved efficacy and isoform selectivity.

Molecular Pharmacology Fast Forward. Published on September 1, 2016 as DOI: 10.1124/mol.116.105437
This article has not been copyedited and formatted. The final version may differ from this version.

Acknowledgements

The authors would like to thank Sally Stoehr for help with initial experiments; Eva Prazak and Doug McIlvaine for providing cells, and Neil Castle and Doug Krafte for their suggestions during the drafting of the manuscript.

Molecular Pharmacology Fast Forward. Published on September 1, 2016 as DOI: 10.1124/mol.116.105437
This article has not been copyedited and formatted. The final version may differ from this version.

Authorship contributions:

Participated in research design: Theile, Fuller, Chapman

Conducted experiments: Theile, Fuller

Contributed new reagents or analytical tools:

Performed data analysis: Theile, Fuller, Chapman

Wrote or contributed to the writing of the manuscript: Theile, Chapman

Molecular Pharmacology Fast Forward. Published on September 1, 2016 as DOI: 10.1124/mol.116.105437
This article has not been copyedited and formatted. The final version may differ from this version.

References

Ahuja S, Mukund S, Deng L, Khakh K, Chang E, Ho H, Shriver S, Young C, Lin S, Johnson JP Jr, *et al.* (2015) Structural basis of Nav1.7 inhibition by an isoform-selective small-molecule antagonist. *Science* **350**: aac5464-1-aac5464-9.

Alexandrou AJ, Brown AR, Chapman ML, Estacion M, Turner J, Mis M, Wilbrey A, Payne CE, Gutteridge A, Cox P, *et al.* (2016) Subtype-selective small molecule inhibitors reveal a fundamental role for Nav1.7 in nociceptor electrogenesis, axonal conduction and presynaptic release. *PLoS One*. e0152405.

Bezanilla F, Taylor RE, and Fernandez JM (1982) Distribution and kinetics of membrane dielectric polarization. 1. Long-term inactivation of gating currents. *J Gen Physiol* **79**: 21-40.

Capes DL, Goldschen-Ohm MP, Arcisio-Miranda M, Bezanilla F, and Chanda B (2013) Domain IV voltage-sensor movement is both sufficient and rate limiting for fast inactivation in sodium channels. *J Gen Physiol* **142**: 101-112.

Catterall WA (2000) From ionic currents to molecular mechanisms: the structure and function of voltage-gated sodium channels. *Neuron* **26**: 13-25.

Catterall WA (2010) Ion channel voltage sensors: structure, function, and pathophysiology. *Neuron* **67**: 915-928.

Catterall WA, Cestele S, Yarov-Yarovoy V, Yu FH, Konoki K, and Scheuer T (2007) Voltage-gated ion channels and gating modifier toxins. *Toxicon* **49**: 124-141.

Cox JJ, Reimann F, Nicholas AK, Thornton G, Roberts E, Springell K, Karbani G, Jafri H, Mannan J, Raashid Y, *et al.* (2006) An SCN9A channelopathy causes congenital inability to experience pain. *Nature* **444**: 894-898.

Cummins TR, and Rush AM (2007) Voltage-gated sodium channel blockers for the treatment of neuropathic pain. *Expert Rev Neurother* **7**: 1597-1612.

Dib-Hajj SD, Black JA, and Waxman SG (2009) Voltage-gated sodium channels: therapeutic targets for pain. *Pain Med* **10**: 1260-1269.

Dib-Hajj SD, Yang Y, and Waxman SG (2008) Genetics and molecular pathophysiology of Na(v)1.7-related pain syndromes. *Adv Genet* **63**: 85-110.

Errington AC, Stohr T, Heers C, and Lees G (2008) The investigational anticonvulsant lacosamide selectively enhances slow inactivation of voltage-gated sodium channels. *Mol Pharmacol* **73**: 157-169.

Groome JR (2014) The voltage sensor module in sodium channels. *Handbook of experimental pharmacology* **221**: 7-31.

Hanck DA and Sheets MF (2007) Site-3 toxins and cardiac sodium channels. *Toxicon* **49**: 181-193.

Hildebrand ME, Smith PL, Bladen C, Eduljee C, Xie JY, Chen L, Fee-Maki M, Doering CJ, Mezeyova J, Zhu Y, *et al.* (2011) A novel slow-inactivation-specific ion channel modulator attenuates neuropathic pain. *Pain* **152**: 833-843.

Hodgkin AL and Huxley AF (1952) A quantitative description of membrane current and its application to conduction and excitation in nerve. *J Physiol* **117**: 500-544.

Jo S and Bean BP (2011) Inhibition of Neuronal Voltage-Gated Sodium Channels by Brilliant Blue G. *Mol Pharmacol* **80**: 247-257.

Karoly R, Lenkey N, Juhasz AO, Vizi ES, and Mike A (2010) Fast- or slow-inactivated state preference of Na+ channel inhibitors: a simulation and experimental study. *PLoS computational biology* **6**: e1000818.

Lenkey N, Karoly R, Kiss JP, Szasz BK, Vizi ES, and Mike A (2006) The mechanism of activity-dependent sodium channel inhibition by the antidepressants fluoxetine and desipramine. *Mol Pharmacol* **70**: 2052-2063.

McCormack K, Santos S, Chapman ML, Krafte DS, Marron BE, West CW, Krambis MJ, Antonio BM, Zellmer SG, Printzenhoff D, *et al.* (2013) Voltage sensor interaction site for selective small molecule inhibitors of voltage-gated sodium channels. *Proc Natl Acad Sci U S A* **110**: E2724-2732.

Noda M, Shimizu S, Tanabe T, Takai T, Kayano T, Ikeda T, Takahashi H, Nakayama H, Kanaoka Y, Minamino N, *et al.* (1984) Primary structure of Electrophorus electricus sodium channel deduced from cDNA sequence. *Nature* **312**: 121-127.

Payne CE, Brown AR, Theile JW, Loucif AJ, Alexandrou AJ, Fuller MD, Mahoney JH, Antonio BM, Gerlach AC, Printzenhoff DM, *et al.* (2015) A novel selective and orally bioavailable Na 1.8 blocker PF-01247324 attenuates nociception and sensory neuron excitability. *Br J Pharmacol* **172**: 2654-2670.

Molecular Pharmacology Fast Forward. Published on September 1, 2016 as DOI: 10.1124/mol.116.105437
This article has not been copyedited and formatted. The final version may differ from this version.

Ragsdale DS, McPhee JC, Scheuer T, and Catterall A (1994) Molecular determinants of state-dependent block of Na+ channels by local anesthetics. *Science* **265**: 1724-1728.

Ragsdale DS, McPhee, JC, Scheuer T, and Catterall WA (1996) Common molecular determinants of local anesthetic, antiarrhythmic, and anticonvulsant block of voltage-gated Na+ channels. *Proc Natl Acad Sci U S A* **93**: 9270-9275.

Rogers JC, Qu Y, Tanada TN, Scheuer T, and Catterall, WA (1996) Molecular determinants of high affinity binding of alpha-scorpion toxin and sea anemone toxin in the S3-S4 extracellular loop in domain IV of the Na+ channel alpha subunit. *J Biol Chem* **271**: 15950-15962.

Stuhmer W, Conti F, Suzuki H, Wang XD, Noda M, Yahagi N, Kubo H, and Numa S (1989) Structural parts involved in activation and inactivation of the sodium channel. *Nature* **339**: 597-603.

Theile JW and Cummins TR (2011) Recent developments regarding voltage-gated sodium channel blockers for the treatment of inherited and acquired neuropathic pain syndromes. *Frontiers in pharmacology **2***: 54.

Vedantham V and Cannon SC (1998) Slow inactivation does not affect movement of the fast inactivation gate in voltage-gated Na+ channels. *J Gen Physiol* **111**: 83-93.

Wang J, Yarov-Yarovoy V, Kahn R, Gordon D, Gurevitz M, Scheuer T, and Catterall WA (2011) Mapping the receptor site for alpha-scorpion toxins on a Na+ channel voltage sensor. *Proc Natl Acad Sci U S A* **108**: 15426-15431.

Xiao Y, Blumenthal K, and Cummins, TR (2014) Gating-pore currents demonstrate selective and specific modulation of individual sodium channel voltage-sensors by biological toxins. *Mol Pharmacol* **86**: 159-167.

Yarov-Yarovoy V, Brown J, Sharp EM, Clare JJ, Scheuer T, and Catterall WA (2001) Molecular determinants of voltage-dependent gating and binding of pore-blocking drugs in transmembrane segment IIIS6 of the Na(+) channel alpha subunit. *J Biol Chem* **276**: 20-27.

Yarov-Yarovoy V, McPhee JC, Idsvoog D, Pate C, Scheuer T, and Catterall WA (2002) Role of amino acid residues in transmembrane segments IS6 and IIS6 of the Na+ channel alpha subunit in voltage-dependent gating and drug block. *J Biol Chem* **277**: 35393-35401.

Molecular Pharmacology Fast Forward. Published on September 1, 2016 as DOI: 10.1124/mol.116.105437
This article has not been copyedited and formatted. The final version may differ from this version.

Footnotes

a) This work was funded by Pfizer Ltd.

b) This work was presented at the 2015 Biophysical Society meeting in Baltimore, MD (2902-Pos/B332. NAV1.7 INHIBITOR, PF-05089771, INHIBITS FAST- AND SLOW-INACTIVATED CHANNELS WITH SIMILAR AFFINITIES)

c) Reprint requests

Jonathan Theile

4222 Emperor Blvd, Suite 350

Durham, NC 27703

jtheile@icagen.com

Molecular Pharmacology Fast Forward. Published on September 1, 2016 as DOI: 10.1124/mol.116.105437
This article has not been copyedited and formatted. The final version may differ from this version.

Figure Legends

Figure 1: Inhibition of human $Na_v1.7$ by PF-05089771 develops and recovers slowly. A. Representative traces showing the timecourse of inhibition under the three different recording conditions. Inhibition by PF-05089771 was assayed against resting channels (steady holding at -120 mV) and a protocol in which channels were half-inactivated during 8-sec prepulses delivered every 15 seconds from a steady holding voltage of -120 mV (V0.5 of inactivation potential was determined empirically for each cell). The sweep interval for both protocols is 15 s. B. Time course of inhibition for half-inactivated channels was dose-dependent, reaching nearly complete block at both 100 nM (*n*=3) and 1 μM (*n*=9), however block was minimal for resting channels (*n*=4). C. Recovery from block following washout of 1 μM PF-05089771 using the tonic protocol (inset) is slow and incomplete (*n*=5).

Figure 2: Using brief depolarizations, PF-05089771 exhibits use-dependence only at very high concentrations. A. Use-dependent inhibition was examined by employing a standard high frequency pulse train consisting of 100 steps (20 ms) to 0 mV at a rate of 10 Hz. The 10 Hz train was tested against the vehicle control (0.1% DMSO, *n*=24) and PF-05089771 at 100 nM (*n*=5), 1 μM (*n*=5), 3 μM (*n*=5) and 10 μM (*n*=9). B. Following complete block with the 10 Hz train in the presence of 10 μM PF-05089771, recovery was assessed using a tonic protocol (*inset*) while washing out the compound (*n*=8). The gray line is the curve fit from Figure 1C, showcasing the similar rate but different extent of recovery from block.

Molecular Pharmacology Fast Forward. Published on September 1, 2016 as DOI: 10.1124/mol.116.105437
This article has not been copyedited and formatted. The final version may differ from this version.

Figure 3: Timecourse of block by PF-05089771 is independent of the availability of kinetically defined inactivated states. A. Recovery from inactivation was assessed following a conditioning depolarizing pulse to 0 mV for 0.1, 1, 4 and 8 s in the absence of PF-05089771 (*n* = 4, 4, 4 and 5 respectively). A variable recovery interval at -120 mV followed each step to 0 mV. Following the recovery interval, a 10 ms test pulse at 0 mV assessed the fraction of available current. As the conditioning pulse is increased from 0.1 to 8 s, a larger fraction of channels enter a slowly recovering state. B. Individual traces from a single representative cell showing recovery from inactivation following either a 1 s (top traces) or an 8 s (bottom traces) pulse to 0 mV. The pulses represent the recovery intervals from 1 ms to 10 s in half-log intervals. C. Onset of block by 100 nM of PF-05089771 was measured using a short (1 s, *n*=5) or long (8 s, *n*=7) inactivating conditioning pulse to 0 mV using the protocols shown in D. The black dots overlaying the red data points represent the time-matched equivalent at 0 mV compared to blue data points (i.e., every 8 s). D. A fixed recovery interval of 1 and 3 s at -120 mV (which allows for >90% of the current to recover) was used for the 1 and 8 s conditioning pulse, respectively. Sweep intervals of 10 and 20 s were used with the 1 and 8 s conditioning pulses, respectively. E. Re-plotting as the amount of block as a function of the total time spent at 0 mV uncovers a similar time course of inhibition between the two protocols ($\tau = 31 \pm 1$ s vs 32 ± 4 s for the 8 s and 1 s conditioning steps, respectively; $P > 0.05$ by unpaired t-test).

Figure 4: Onset of inhibition develops over similar time course using different conditioning trains with equal time at 0 mV. A. Recovery from inactivation was assessed following a conditioning prepulse train to 0 mV at a frequency of 1 Hz (*n*=5) and 0.1 Hz (*n*=4) in the absence of PF-05089771. B. Onset of block by 100 nM of PF-05089771 (*n*=3, each) was measured

Molecular Pharmacology Fast Forward. Published on September 1, 2016 as DOI: 10.1124/mol.116.105437
This article has not been copyedited and formatted. The final version may differ from this version.

using both protocols but with a fixed recovery interval of 3 s at -120 mV and a sweep interval of 20 s. The onset of block is similar with both protocols (τ = 141 ± 23 s for the 10 x 400 ms, 1 Hz and 178 ± 16 s for the 1 x 4 s, 0.1 Hz, n=3 each; $P > 0.05$ by unpaired t-test), despite the ~3.4 fold difference in relative availability of slow inactivated channels with the 0.1 Hz conditioning stimulus.

Figure 5: Onset of inhibition develops over similar time course from closed- and open-state inactivation. A. Activation and steady-state inactivation curve show minimal overlap. The voltage-dependence of steady-state inactivation (circles) was determined using the protocol shown in (*i*) with a V0.5 of -83.5 $\pm$ 0.5 mV (n=9). The voltage-dependence of activation (squares) was determined using the protocol shown in (*ii*) with a V0.5 of -29.3 $\pm$ 0.3 mV (n=11). B. Recovery from inactivation was assessed following a conditioning pulse at 0 mV (channels inactivated through open-state, *n*=5), -60 mV (channels predominantly inactivated through closed state, *n*=3) or the V0.5 of inactivation (as determined empirically for each cell, *n*=3). For the conditioning pulses to -60 mV and 0 mV, 100% of the channels are inactivated. The rate of recovery for the -60 mV and V0.5 conditioning steps have a considerably larger fast component compared to the conditioning step to 0 mV. Likewise, the recovery from the V0.5 conditioning pulse is predominantly fast. C. Onset of block by 100 nM of PF-05089771 was measured using each protocol with a fixed 3 s recovery interval at -120 mV and a 20 s sweep interval. The rate of block is similar for the 0 mV (*n*=7) and -60 mV (*n*=5) protocols ($P > 0.05$ by ANOVA), despite having dramatically different recovery profiles, however the onset of block is dramatically slower using the V0.5 potential ($P < 0.01$ by ANOVA and Tukey's multiple comparison test, *n*=6).

Molecular Pharmacology Fast Forward. Published on September 1, 2016 as DOI: 10.1124/mol.116.105437
This article has not been copyedited and formatted. The final version may differ from this version.

Tables

Table 1. Best-fit values (for data shown in Figure 3A) using a nonlinear regression with a sum of two exponentials. Tau values were calculated as $1/K_{fast}$ and $1/K_{slow}$. *The tau_{fast} values were constrained to that of the fit for the 0.1 s conditioning pulse.

	0 mV for 0.1 s	**0 mV for 1 s**	**0 mV for 4 s**	**0 mV for 8 s**
A_{fast} (%)	92	70	32	12
Tau_{fast} (ms)	8	8*	8*	8*
A_{slow} (%)	8	30	68	88
Tau_{slow} (ms)	108	326	566	580

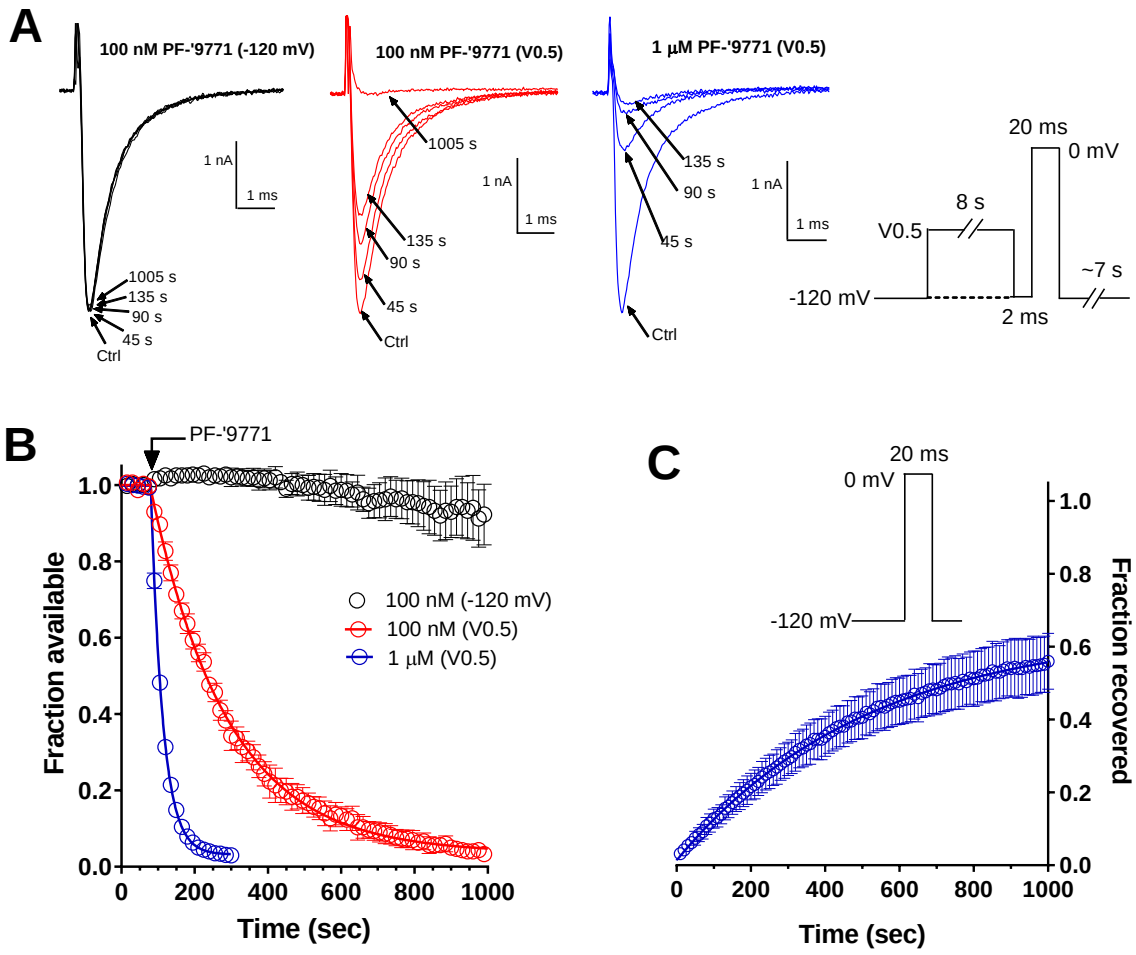
A
100 nM PF-'9771 (-120 mV)
1 nA
1 ms
1005 s
135 s
90 s
45 s
Ctrl
100 nM PF-'9771 (V0.5)
1005 s
135 s
90 s
45 s
Ctrl
1 nA
1 ms
1 µM PF-'9771 (V0.5)
135 s
90 s
45 s
Ctrl
1 nA
1 ms
20 ms
0 mV
8 s
V0.5
~7 s
-120 mV
2 ms
B
PF-'9771
Fraction available
100 nM (-120 mV)
100 nM (V0.5)
1 µM (V0.5)
Time (sec)
C
20 ms
0 mV
-120 mV
Fraction recovered
Time (sec)

Figure 1

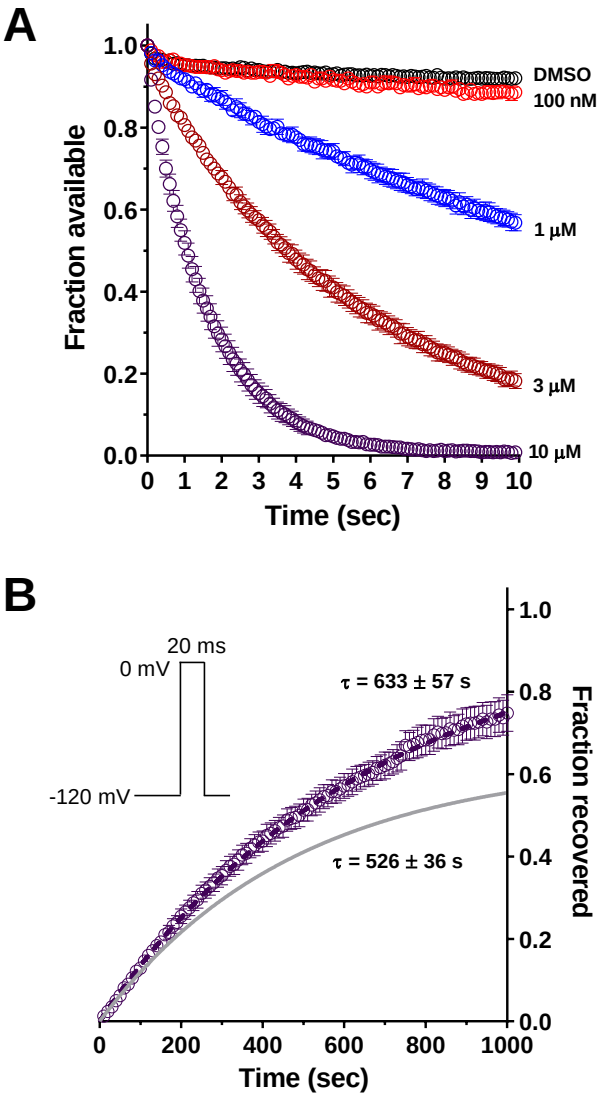
A
Fraction available
Time (sec)
DMSO
100 nM
1 µM
3 µM
10 µM
B
20 ms
0 mV
-120 mV
τ = 633 ± 57 s
τ = 526 ± 36 s
Fraction recovered
Time (sec)

Figure 2

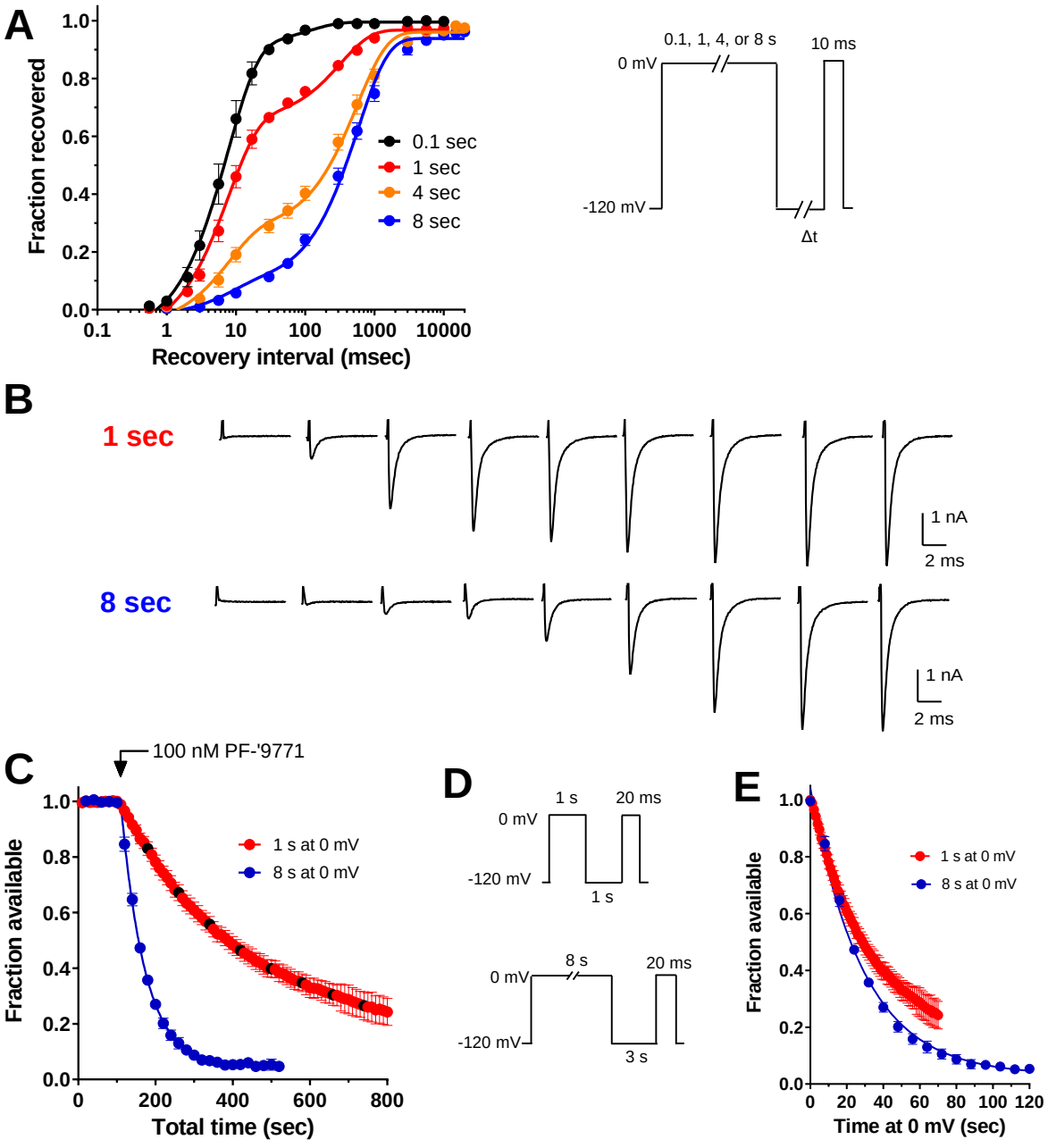
A
Fraction recovered
1.0
0.8
0.6
0.4
0.2
0.0
0.1
1
10
100
1000
10000
Recovery interval (msec)
0.1 sec
1 sec
4 sec
8 sec
0.1, 1, 4, or 8 s
10 ms
0 mV
-120 mV
Δt
B
1 sec
1 nA
2 ms
8 sec
1 nA
2 ms
C
100 nM PF-'9771
Fraction available
1 s at 0 mV
8 s at 0 mV
0
200
400
600
800
Total time (sec)
D
1 s
20 ms
0 mV
-120 mV
1 s
8 s
20 ms
0 mV
-120 mV
3 s
E
Fraction available
1 s at 0 mV
8 s at 0 mV
0
20
40
60
80
100
120
Time at 0 mV (sec)

Figure 3

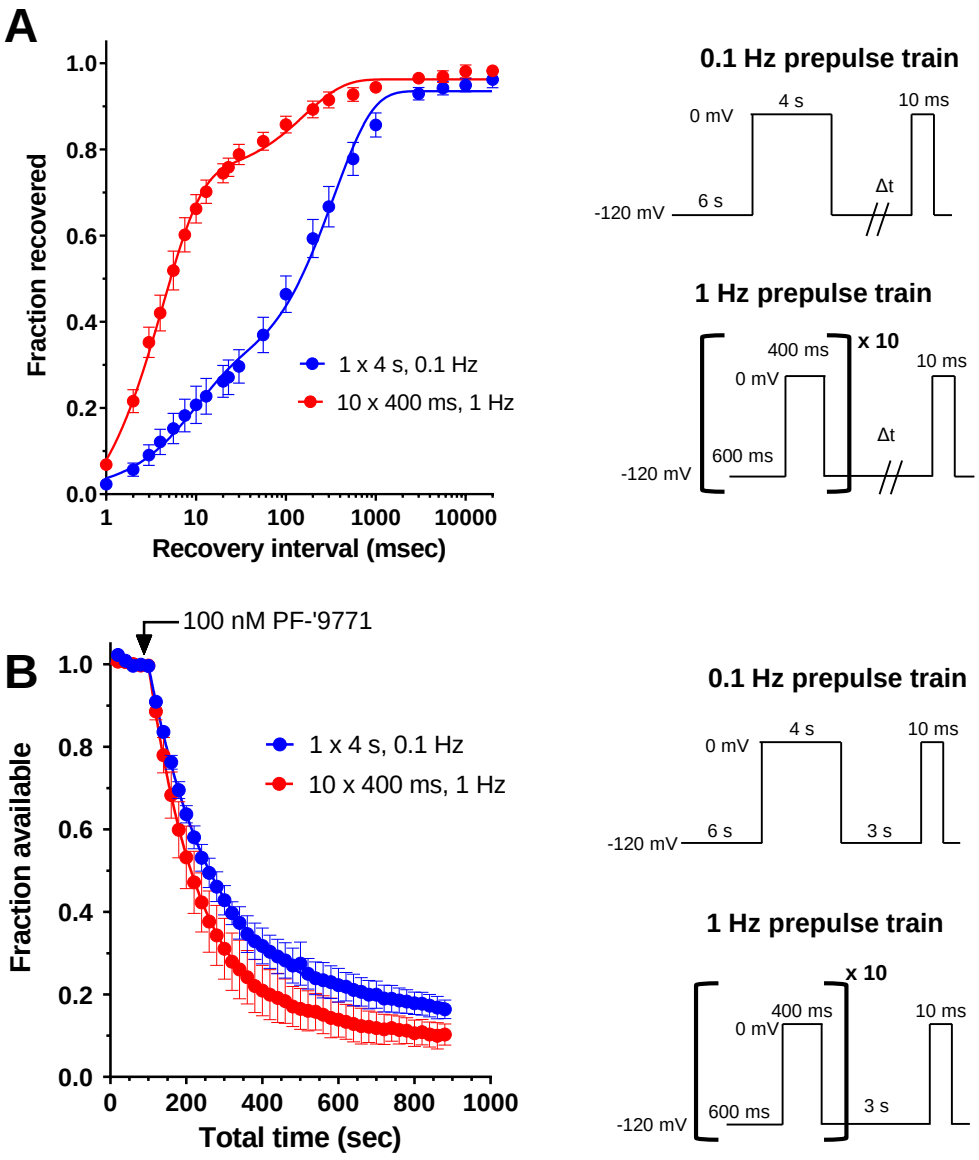
A
Fraction recovered
1.0
0.8
0.6
0.4
0.2
0.0
1
10
100
1000
10000
Recovery interval (msec)
1 x 4 s, 0.1 Hz
10 x 400 ms, 1 Hz
0.1 Hz prepulse train
0 mV
4 s
10 ms
-120 mV
6 s
Δt
1 Hz prepulse train
400 ms
x 10
10 ms
0 mV
600 ms
Δt
-120 mV
B
100 nM PF-'9771
Fraction available
1.0
0.8
0.6
0.4
0.2
0.0
0
200
400
600
800
1000
Total time (sec)
1 x 4 s, 0.1 Hz
10 x 400 ms, 1 Hz
0.1 Hz prepulse train
0 mV
4 s
10 ms
-120 mV
6 s
3 s
1 Hz prepulse train
x 10
400 ms
10 ms
0 mV
600 ms
3 s
-120 mV

Figure 4

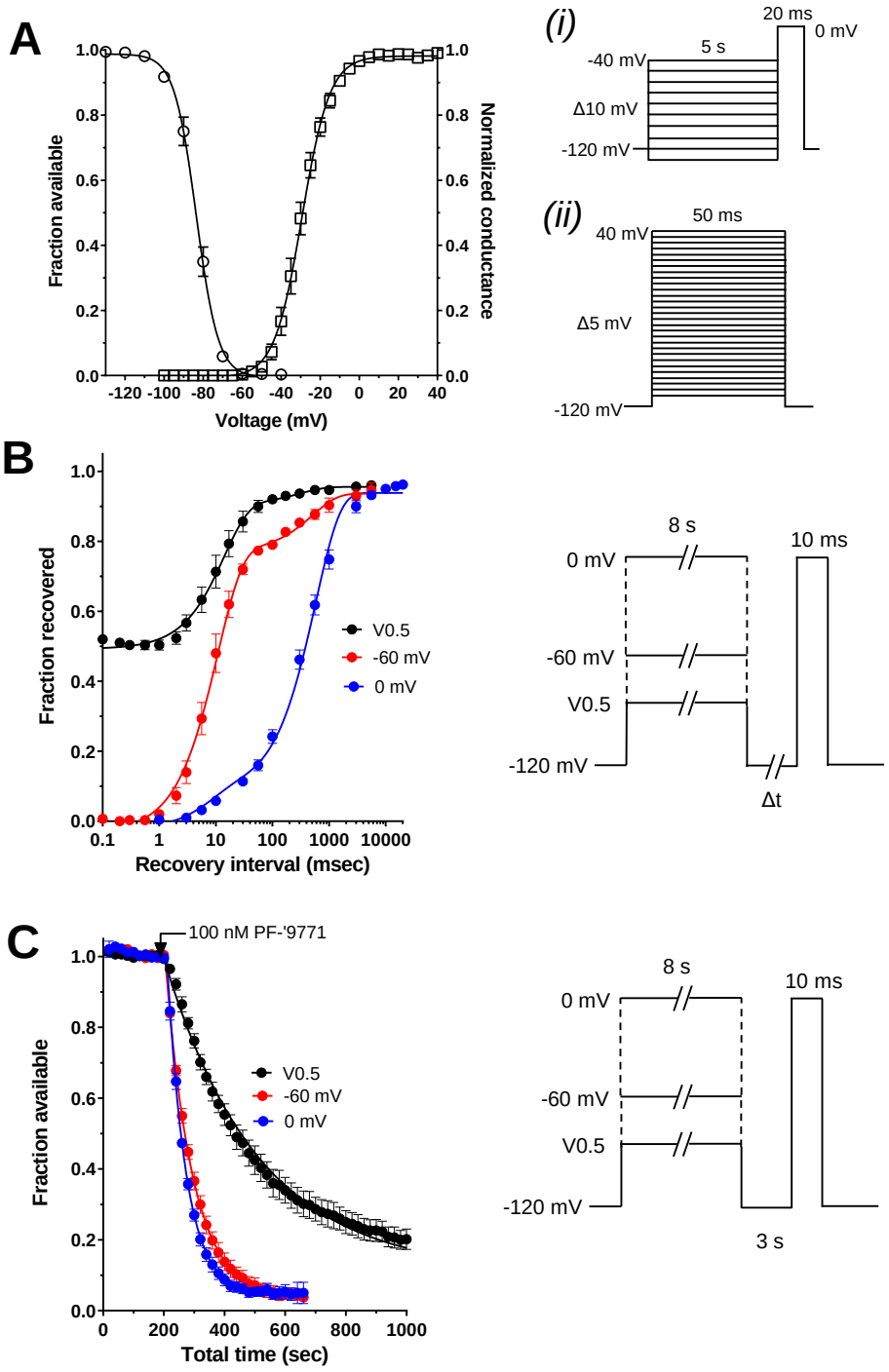
A
Fraction available
Normalized conductance
Voltage (mV)
(i)
20 ms
0 mV
5 s
-40 mV
Δ10 mV
-120 mV
(ii)
50 ms
40 mV
Δ5 mV
-120 mV
B
Fraction recovered
V0.5
-60 mV
0 mV
Recovery interval (msec)
8 s
10 ms
0 mV
-60 mV
V0.5
-120 mV
Δt
C
100 nM PF-'9771
Fraction available
V0.5
-60 mV
0 mV
Total time (sec)
8 s
10 ms
0 mV
-60 mV
V0.5
-120 mV
3 s

Figure 5